

Jason J. Gorman<sup>1</sup>, Yong-Sik Kim<sup>1</sup>, Andras E. Vladar<sup>2</sup> and Nicholas G. Dagalakis<sup>1</sup>

<sup>1</sup>Intelligent Systems Division  
<sup>2</sup>Precision Engineering Division  
National Institute of Standards and Technology  
Gaithersburg, MD 20899  
contact: gorman@nist.gov

### INTRODUCTION

This paper discusses the design of a novel micro-scale nanoassembly system that is intended for both prototyping nanodevices, and high-yield parallel nanomanufacturing. Most precision equipment currently used in nanomanufacturing is large, bulky and expensive. However, microelectromechanical systems (MEMS) present an excellent opportunity to drastically reduce the size and cost of nanomanufacturing equipment by designing fully integrated nanomanufacturing workcells on a single silicon chip. The reduction in size would enable parallel manufacturing while the reduced cost would significantly widen access to nanomanufacturing equipment. Furthermore, retooling these systems would only involve redesign and fabrication at minimal cost compared to overhauling macro-scale equipment.

The use of MEMS for nanotechnology research has recently achieved acceptance by a number of researchers. MEMS nanopositioning mechanisms for ultra-precision motion applications have been developed by Bergna et al. [1], and Chen and Culpepper [2]. Other micro-scale instruments that have been demonstrated include a micro-AFM [3] and an atomic trapping and cooling apparatus [4]. In all of these examples, the main challenge in scaling down the critical dimensions of an instrument is to maintain the same level of operational precision of the equivalent macro-scale instrument. Limits in microfabrication processes, viable materials, and tolerances make this challenge particularly difficult. Therefore, it is important that the benefits of reduced size and cost, among others, are weighed against the difficulties in achieving nano-scale precision with micro-scale mechanisms.

In this paper, the design and proposed operation of a MEMS-based nanoassembly system is presented. The nanoassembly system is comprised of four nanomanipulators that can work independently or cooperatively. The design of the nanomanipulators will be discussed and experimental characterization results for one nanomanipulator will be presented. Three critical research issues for this project are then discussed: nanomanipulation strategies using the nanoassembly system; MEMS precision motion control; and integration of the on-chip nanoassembly system with a scanning electron microscope / focused ion beam instrument to obtain a complete nanomanufacturing environment.

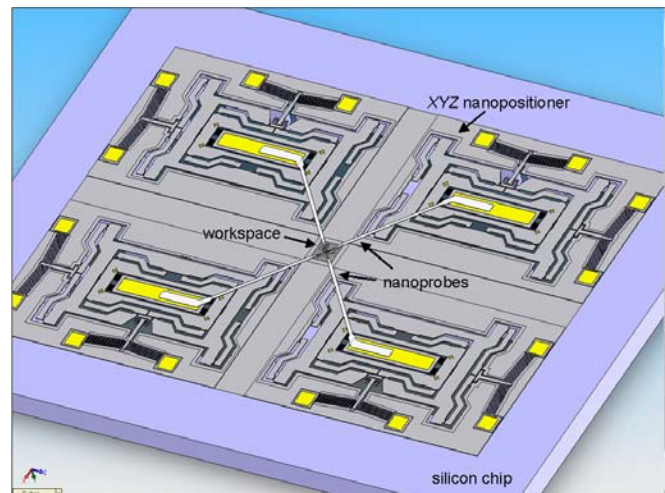


Fig. 1 Micro-scale nanoassembly cell with 2 x 2 array of XYZ nanomanipulators

### PROPOSED SYSTEM DESIGN

One of the main thrusts of nanotechnology research has been the design and fabrication of nano-scale structures with unique physical properties. Structures such as carbon nanotubes, semiconducting nanowires and quantum dots have been investigated by numerous researchers and many intriguing nanodevices composed of these structures have been proposed. However, few of these devices, if any, have been implemented with reliability or functionality typical of commercialized components. A major challenge in nanomanufacturing is to establish methods of manufacturing based around these nanostructures that will enable high-yield production. Critical processes that need to be developed include nanostructure extraction, cutting, bonding, manipulation, and assembly.

Manipulation and assembly at the nano-scale is a particularly challenging problem that has received only limited attention. Carbon nanotubes have been successfully manipulated using an atomic force microscope (AFM) for structural experiments by Yu et al. [5]. The mechanical interactions between an AFM tip and nanoparticles during manipulation on a substrate have been modeled and utilized to improve manipulation by Sitti and Hashimoto [6]. This manipulation approach has also been extended to include the assembly of polymer nanoparticles and their subsequent

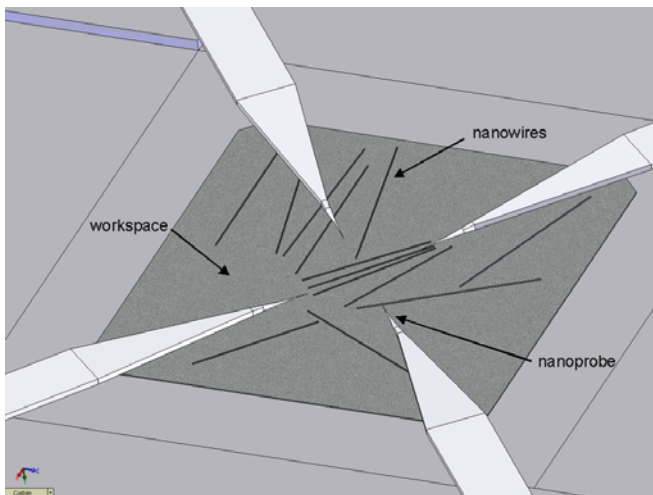


Fig. 2 Multiple nanoprobes working in a shared workspace

thermal bonding [7]. Although AFMs are capable of nanomanipulation and are an obvious choice due to their widespread availability, they have many limitations as a nanomanipulator. Most importantly, they are generally limited to a single probe with three degrees of freedom. Furthermore, the AFM cantilever occludes the manipulation maneuvers, making it difficult to utilize visual feedback from a scanning electron microscope (SEM).

An improved but similar approach to AFM nanomanipulation is the use of a sharp tipped nanoprobe that can be positioned with nanometer resolution, as has been demonstrated for micromanipulation by Kasaya et al. [8]. In this case, the manipulation of nanostructures can be visualized with an SEM without occlusion while the basic approach of AFM nanomanipulation, pushing with the tip of a sharp probe, is maintained. Based on this concept, we have proposed a micro-scale multi-nanoprobe nanoassembly system based on microsystems technology.

A schematic of the proposed micro-scale nanoassembly system is shown in Fig. 1. The system is composed of four XYZ MEMS nanopositioners that are arranged in a 2 x 2 array. Each nanopositioner has a single nanoprobe attached, creating a nanomanipulator similar in functionality to an AFM. The four nanomanipulators share a common workspace at the center of the array where nanostructure samples can be introduced, as shown in Fig. 2. By coordinating the motion of all four nanomanipulators, complex nanoassembly functionalities can be achieved. Parallel nanoassembly, as well as assembly line approaches, are possible by increasing the size of the array.

As a first step in this project, we have designed and fabricated a 2 x 2 array of XYZ MEMS nanopositioners based on the nanopositioning mechanisms presented in [1]. One of these prototypes is shown in Fig. 3. The X and Y axes are actuated by bent-beam thermal actuators, which were chosen due to their high stiffness and large output force. These actuators apply forces along their respective axes to the flexure mechanism, resulting in displacement of the center stage. The flexure mechanism design utilizes a parallel dual-lever to amplify the motion along the axis of desired

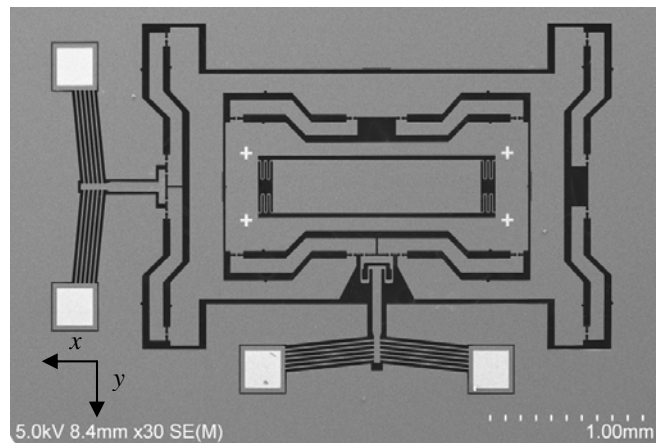


Fig. 3 Fabricated micro-scale XYZ nanomanipulator

motion while minimizing crosstalk between the X and Y axes. Motion along the Z axis is generated by applying a force to the center plate, which is supported by four serpentine springs. Both electromagnetic and electrostatic actuator prototypes have been designed for driving this degree of freedom. We are currently working on integrating these actuator schemes into the prototype.

#### MECHANISM CHARACTERIZATION

The XYZ nanopositioner discussed in the previous section is a critical element in the nanoassembly system and must perform manipulation maneuvers with nano-scale precision. In this section we discuss some initial experimental characterization results for this mechanism. First, results for the static calibration of the relationship between the input voltage and resulting displacement of the mechanism are discussed. Then results on the crosstalk between the X and Y axes is presented. Finally, measurements of system frequency responses are discussed.

The quasi-static relationship between the mechanism displacement and input voltage was measured using an optical microscope with a digital camera. The input voltage was varied and at each input voltage an image was captured at 100X magnification. Applying image processing to the sequence of images for the X and Y axes results in the data shown in Figs. 4 and 5. In general, the behavior of the mechanism is as expected, where the displacement is a quadratic function of the input voltage. This is due to the fact that the temperature of the actuator is a function of the power dissipation caused by Joule heating. It was found that for a voltage range of 0 V to 10 V, the displacement was 5.0  $\mu\text{m}$  along the X axis and 3.4  $\mu\text{m}$  along the Y axis. These values are significantly smaller than those found for a 1 degree of freedom (DOF) mechanism of similar dimensions [1]. This is likely due to a change in stiffness of the flexure mechanism due to coupling between the X and Y axes. Additionally, the data shows that the mechanism strays from the quadratic behavior at 10 V for both axes, indicating that there may be some electrical coupling in the mechanism that is causing the reduced displacement. Optimization of the flexure mechanism for increased range will be explored in the future

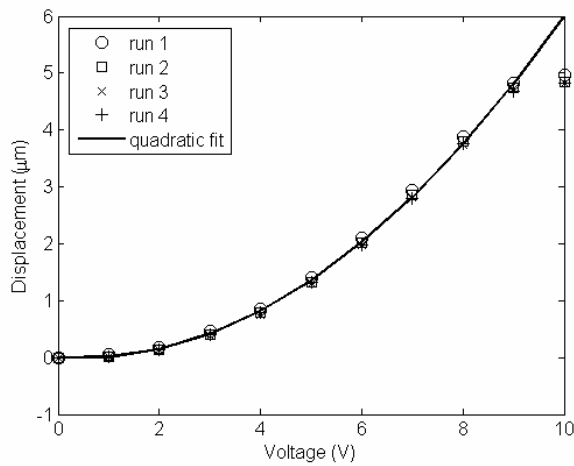


Fig. 4 Displacement vs. input voltage for X axis

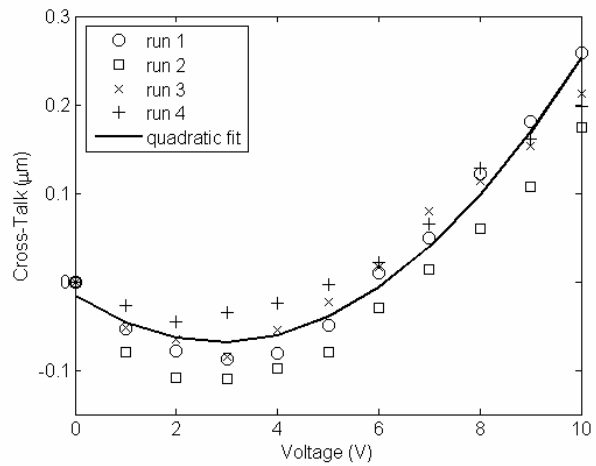


Fig. 6 Crosstalk along Y axis when input voltage is applied to X axis

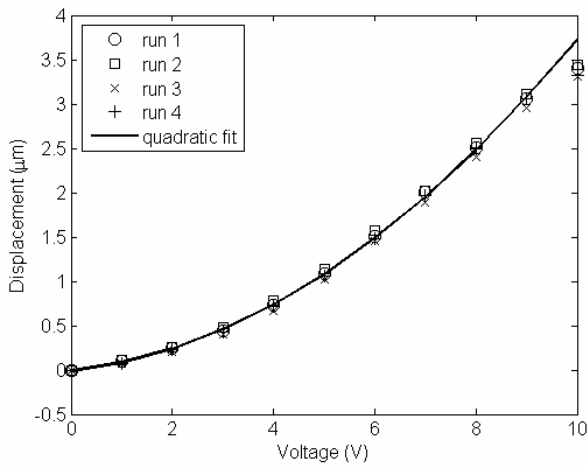


Fig. 5 Displacement vs. input voltage for Y axis

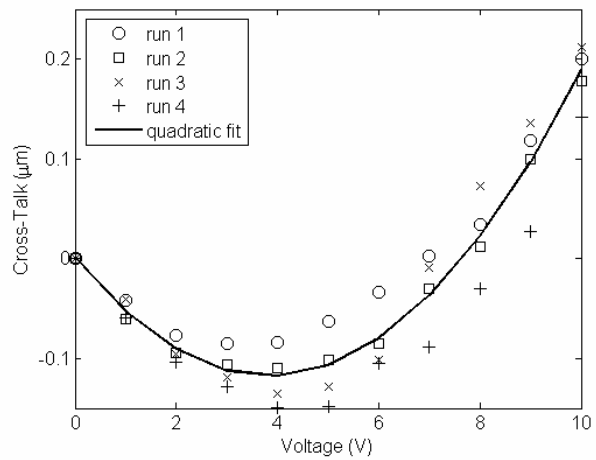


Fig. 7 Crosstalk along X axis when input voltage is applied to Y axis

and we are currently investigating methods for electrically isolating individual axes.

As mentioned previously, the X and Y axes are mechanically coupled through the flexure mechanism. Therefore, coupled motion is expected, otherwise known as crosstalk. The crosstalk between these axes was measured by actuating one axis while measuring the displacement of the orthogonal axis using the method described above. The crosstalk as a function of input voltage in the X and Y axes for a voltage range of 0 V to 10 V is shown in Figs. 6 and 7. The maximum crosstalk was found to be approximately 220 nm and 250 nm in the X and Y directions, respectively. Additionally, the data shows that the crosstalk follows a quadratic curve that is not centered about the origin. Comparing this result to the displacement data in Figs. 4 and 5, the percentage crosstalk for full range displacement is 6.1 %. Although this result is not optimal, this level of coupling could be calibrated out and the effect on the manipulation precision would likely not be an issue.

Finally, the frequency response of the mechanism was measured to understand the actuator bandwidth and to determine the effects of resonance on the mechanism's motion. The frequency responses were measured using the swept-sine method and a laser reflectance microscope which

provides an in-plane measurement of the motion of the mechanism, as discussed in [9]. Since the thermal actuator response is nonlinear, the measurements were performed with a 5 V bias in the input voltage and a small excitation signal (~500 mV pk-pk). Both the actuator and mechanism response were measured for the X and Y axes. Figure 8 shows the frequency response of the thermal actuator and the entire mechanism for the X axis. Since the flexure mechanism amplifies the motion of the actuator, the motion of the flexure mechanism is larger than the thermal actuator. However, for the purpose of comparison, the frequency responses have been normalized. This data clearly shows that the system dynamics are a combination of a first-order response due to the thermal actuator, and the structural modes of the flexure mechanism. In general, the response for the actuator is similar to the overall mechanism. The useable bandwidth of the mechanism is approximately 65 Hz.

The frequency responses along the Y axis demonstrate a fundamental difference, as shown in Fig. 9. Here the response of the actuator is free of any resonances, while the measurement for the entire mechanism is shown to have a resonance. This is most likely due to the fact that the Y axis is designed to be decoupled from the X axis when the X axis displacement is zero. However, the X axis is not decoupled

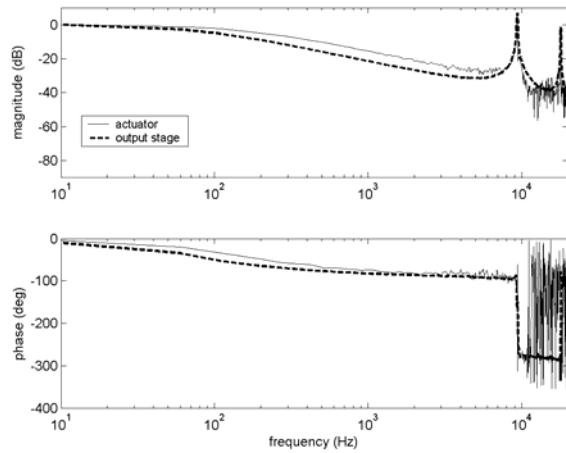


Fig. 8 Experimental frequency response for X axis

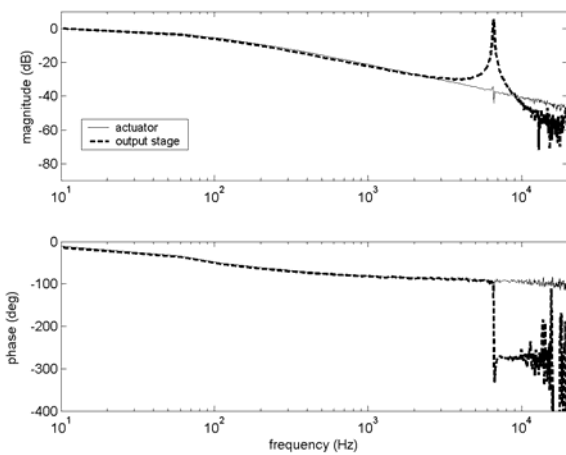


Fig. 9 Experimental frequency response for Y axis

from the Y axis, even when the Y axis displacement is zero. This coupling can be seen in Fig. 3, where the Y axis actuator clearly causes a moment on the flexure mechanism when the X axis displaces. The working bandwidth for the Y axis was determined to be approximately 42 Hz.

The dynamic response of the mechanism is critical to its performance in nanomanipulation because it determines the fastest rate at which the nanomanipulator can move without vibration. Similar to the results in [9], in the future we will apply a nonlinear model to this data and then design a closed-loop controller that will maximize this bandwidth while maintaining nano-scale position resolution.

### CRITICAL RESEARCH ISSUES

The design of the on-chip nanoassembly system is only the first step in implementing a precision nanoassembly environment. In addition to our research on the proposed mechanism, a number of problems must be solved including the development of repeatable manipulation maneuvers using multiple nanoprobes; precision motion control; and the integration of the nanoassembly system within a scanning electron microscope / focused ion beam (SEM/FIB) instrument. Some of our plans for addressing these problems are discussed in the following subsections.

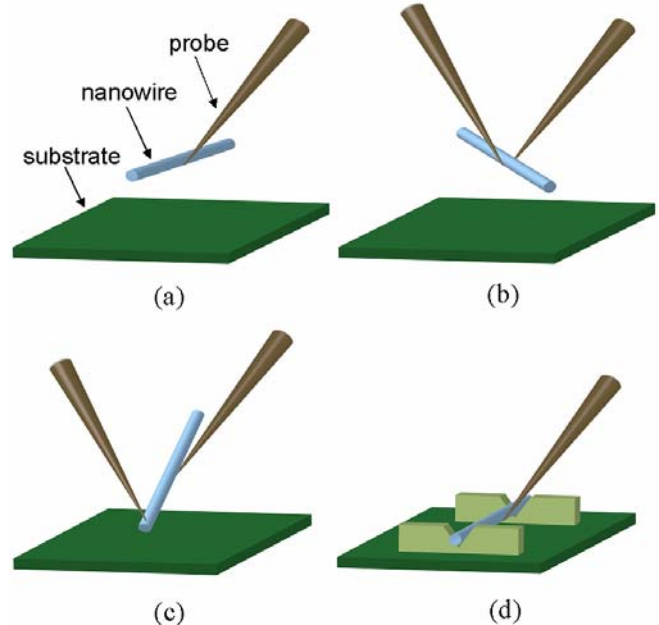


Fig. 10 Nanomanipulation of a nanowire using nanoprobes. (a) manipulation via adhesion, (b) manipulation via gripping, (b) rotating a nanowire with two nanoprobes, (d) assembly using v-notch fixtures.

### A. MANIPULATION STRATEGIES

Manipulating nano-scale structures is particularly challenging since surface forces, including van der Waals, electrostatic and capillary forces, dominate the dynamics at this scale. In general, the motion of a nanostructure when pushed along a surface is not deterministic because surface forces are inhomogeneous due to variations in surface roughness, charge and water adsorption. Therefore, successful manipulation schemes must be developed which constrain the manipulated nanostructure for deterministic motion in an inhomogeneous force field while also minimizing the contact area between the nanostructure and manipulation tools. We intend to address this problem by designing specific manipulation primitives and developing simulation models for verifying the manipulation strategies offline.

Implementing manipulation schemes with nanoprobes as manipulations tools minimizes the contact area between the tool and nanostructure, and provides a number of useful and interesting functionalities. Using a single nanoprobe, a nanostructure can be pushed on a surface for planar assembly, and under the proper environmental conditions can be manipulated in three dimensions by utilizing adhesion (Fig. 10a). As mentioned previously, using only a single nanoprobe is difficult due to inhomogeneous surface forces, but the approach works in some situations.

Multiple nanoprobe manipulation strategies are needed to properly constrain a nanostructure during assembly. Two nanoprobes can be used as tweezers for grabbing a single nanostructure (Fig. 10b). They can also be used for three dimensional operations such as rotating a nanostructure (Fig. 10c). This can be extended to three nanoprobes, where two are used to grip the nanostructure while the third is used to

rotate the nanostructure about its gripping point. Since adhesion can hinder the release of nanostructures when assembling a device, simple and repeatable methods for accurate placement are needed. The most straightforward approach is to use nanofabricated fixtures such as v-notches (Fig. 10d). Here, the adhesion forces are dominated by the contact forces, yielding a repeatable release.

### B. PRECISION MOTION CONTROL

Precision motion control of these mechanisms is critical for successful nanoassembly. An open-loop control approach has been developed to achieve motion resolution on the order of nanometers by calibrating the input (voltage) – output (displacement) relationship of the mechanism and then inverting this relationship to calculate the required control voltage for a desired motion profile. As an example of the motion resolution that can be achieved using this approach, a prototype nanomanipulator was controlled to perform 50 nm steps, as shown in Fig. 11. The motion was measured in an SEM and the resolution was found to be smaller than  $\pm 7$  nm. Although this level of control would be acceptable, the open-loop approach has been found to only be repeatable within a small range, and errors become unacceptable for larger excursions.

Closed-loop control is currently being explored so that nano-scale precision can be achieved over the entire range. First, position sensors must be included in the mechanism design. Although capacitive sensors typically have the best resolution and stability, a comb structure with the required capacitance is likely to be larger than would be acceptable for the nanoassembly array. Therefore, we are also currently working on the design of piezoresistive position sensors. With the addition of feedback, the nonlinear PID controller discussed in [9] will then be implemented.

### C. SEM/FIB INTEGRATION

Upon completion of the nanoassembly system, the necessary integration for operation within an SEM/FIB will be performed. The long term goal of this project is to combine nanoassembly, nano-scale imaging, and FIB material deposition and milling into a stand-alone nanomanufacturing system. Although FIB deposition and milling are now common approaches in nanotechnology research [10], there are still many issues to be resolved in order to utilize these approaches with a level of precision and repeatability expected of a nanomanufacturing system. Additionally, the interactions between the nanoassembly system and SEM/FIB system will present many new challenges.

One prototype assembly operation that highlights many of the processes that will be handled by this nanomanufacturing system is the assembly of a nanowire resonator. A nanowire is first manipulated to isolate it from other structures. The FIB is then used to cut the nanowire to the proper size. Then, the nanowire is placed across two electrical contacts using the nanoassembly system. Platinum is then deposited over the ends of the nanowire to bond it to the contacts using the FIB. Finally, the nanoassembly system can be used to probe the nanowire device for electrical and mechanical measurements. Within this process there are a number of issues that must be

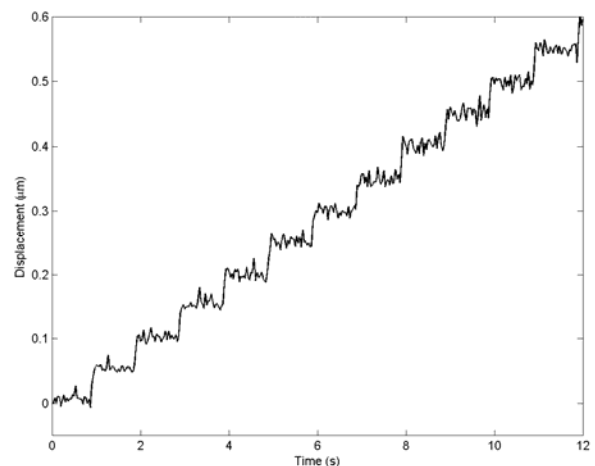


Fig. 11 Open-loop nanopositioning of a prototype nanomanipulator (50 nm steps)

explored for repeatable manufacturing. In particular, the interactions between the FIB and the nanoassembly system, such as contamination of the nanoprobe with precursor components, will be investigated. Furthermore, the mechanical and electrical quality of platinum deposition for nanowire bonding requires further investigation [11,12].

### CONCLUSION

This paper has discussed a proposed design for an on-chip nanoassembly system that is currently under development. A prototype nanomanipulator has been fabricated and its static and dynamic motion behavior has been characterized. The mechanism appears to be suitable for nanoassembly and is being redesigned for increased motion range. Additional research objectives have also been outlined that are critical for the success of this project including manipulation strategies, precision motion control and integrating the nanoassembly system with an SEM/FIB. If successful, this project will result in an on-chip nanomanufacturing system that would be the first of its kind.

### REFERENCES

- [1] S. Bergna, J. J. Gorman, and N. G. Dagalakis, "Design and modeling of thermally-actuated MEMS nanopositioners," *Proceedings of the ASME IMECE*, Orlando, FL, 2005, IMECE2005-82158.
- [2] S.-C. Chen and M. L. Culpepper, "Design of a six-axis micro-scale nanopositioner -  $\mu$ HexFlex," *Precision Engineering*, vol. 30, pp. 314-324, 2006.
- [3] Y. Xu, N. C. MacDonald, and S. A. Miller, "Integrated micro-scanning tunneling microscope," *Applied Physics Letters*, vol. 67, pp. 2305-2307, 1995.
- [4] C. O. Gollasch, Z. Mektadir, M. Kraft, M. Trupke, S. Eriksson, and E. A. Hinds, "A three-dimensional electrostatic actuator with a locking mechanism for microcavities on atom chips," *Journal of Micromechanics and Microengineering*, vol. 15, pp. S39-S46, 2005.
- [5] M.-Y. Yu, M. J. Dyer, G. D. Skidmore, H. W. Rohrs, X.-K. Lu, K. D. Ausman, J. R. Von Her, and R. S. Ruoff, "Three-dimensional manipulation of carbon nanotubes under a scanning electron microscope," *Nanotechnology*, vol. 10, pp. 244-252, 1999.
- [6] M. Sitti and H. Hashimoto, "Controlled Pushing of Nanoparticles: Modeling and Experiments," *IEEE/ASME Transactions on Mechatronics*, vol. 5, pp. 199-211, 2000.
- [7] E. Harel, S. E. Meltzer, A. A. G. Requicha, M. E. Thompson and B. E. Koel, "Fabrication of polystyrene latex nanostructures by

- nanomanipulation and thermal processing," *Nanoletters*, Vol. 5, pp. 2624-2629, 2005.
- [8] T. Kasaya, H. T. Miyazaki, S. Saito, K. Koyano, T. Yamaura, and T. Sato, "Image-based autonomous micromanipulation system for arrangement of spheres in a scanning electron microscope," *Review of Scientific Instruments*, Vol. 75, pp. 2033-2042, 2004.
- [9] J. J. Gorman, Y.-S. Kim, and N. G. Dagalakis, "Control of MEMS nanopositioners with nano-scale resolution," *Proceedings of the ASME IMECE*, Chicago, IL, 2006, IMECE2006-16190.
- [10] S. Reynjtjens and R. Puers, "A review of focused ion beam applications in microsystems technology," *Journal of Micromechanics and Microengineering*, Vol. 11, pp. 287-300, 2001.
- [11] S. B. Cronin, Y.-M. Lin, O. Rabin, M. R. Black, J. Y. Ying, M. S. Dresselhaus, P. L. Gai, J.-P. Minet, and J.-P. Issi, "Making electrical contacts to nanowires with a thick oxide coating," *Nanotechnology*, Vol. 13, pp. 653-658, 2002.
- [12] C. Y. Nam, J. Y. Kim, and J. E. Fischer, "Focused-ion-beam platinum nanopatterning for GaN nanowires: Ohmic contact and patterned growth," *Applied Physics Letters*, Vol. 86, 193112, 2005.